Astron. Astrophys. 176, 358–366 (1987)

ASTRONOMY
AND
ASTROPHYSICS

The nature of two anomalous structures observed in the dust tail of Comet Bennett 1970 II: a possible Neck-Line Structure

L. Pansecchi [1], **M. Fulle** [2], **and G. Sedmak** [2,3]

[1] Osservatorio San Vittore, Via San Vittore 44, I-40136 Bologna, Italy
[2] ISAS-International School for Advanced Studies, Strada Costiera 11, I-34014 Trieste, Italy
[3] Università di Trieste, Dipartimento di Astronomia, Via G. Tiepolo 11, I-34100 Trieste, Italy

Received November 18, 1985; accepted December 15, 1986

Summary. Three red-light photographs of Comet Bennett 1970II, taken at the Karl Schwarzschild Observatory, Tautenburg close to the date of the Earth passage through the comet nodal line, are presented. All the plates show an anomalous ray-shaped structure (RSS) stretching from the nucleus across a regular, edgewise-seen, dust tail, and a short sunward spike (SWS), strongly recalling that of Comet Tago-Sato-Kosaka 1969IX. The shape and the behaviour of the RSS during the relevant time strongly recall the sunward spike of Comet Arend-Roland 1957III observed under similar geometrical circumstances (although here the RSS is oriented in the direction opposite to the Sun, as the main tail). The spectral range of the observations, and other circumstantial proofs allow to consider such features as dusty structures. Image processing is developed in order to enhance the low visibility of the SWS, partly embedded in the coma. The classical explanation, based on the meteoric swarm, could explain, as in the case of Comet Arend-Roland, the RSS, but the only realistic model which can explain both the structures is the NLS model developed by Kimura and Liu (1977) using the rigorous treatment of the motion of the comet tail dust grains. A new complete model of these two-dimensional structures is developed, whose results are able to explain the observations. In order to account for the shape and extension of the SWS, a dust ejection velocity from the inner coma $\geqq 0.03\ \mathrm{km\ s^{-1}}$ is required, in disagreement with the hypothesis of zero velocity release assumed in the meteoric swarm model.

Key words: celestial mechanics – comets – image processing

1. Introduction

Three red light photographs of Comet Bennett 1970II, taken at the Karl Schwarzschild Observatory, Tautenburg nearly at the time of the Earth passage through the plane of the comet orbit, show two anomalous structures in the tail of the comet. The first is a ray-shaped structure (RSS) stretching from the nucleus across a regular, edgewise-seen dust tail. The second is a short sunward spike (SWS), strongly resembling the sunward spike of Comet Tago-Sato-Kosaka 1969IX (Miller et al., 1971), although somewhat fainter. This paper is devoted to the physical interpretation of these features, which could satisfy a model of dusty structures which allows new investigations of the cometary dust size distribution and ejection velocity (Fulle and Sedmak, 1986). The physical interpretation of the features and the astrometric measurements are due to L. P., the mathematical model to M. F. and the image processing to G. S.

Send offprint requests to: M. Fulle

2. The observations

2.1. *The Tautenburg photographs*

The present study was performed on contact prints on plan film of the original plates (24 × 24 cm in size, $51''.6\ \mathrm{mm^{-1}}$) made available to us by Prof. Richter. We could analyse a total of five plates taken at Tautenburg Observatory near the date of the Earth passage through the comet nodal line (Högner and Richter, 1980). Three of them (plates 3124, 3125, and 3127) are 103a-E panchromatic emulsions combined with an RG1 filter to cut off wavelengths below ≈6000 Å and thereby to suppress efficiently most plasma features of the tail. The other two plates, taken about 1 h before observations 3124 and 3127, are standard 103a-O emulsions with UG2 filter showing the Type I (plasma) component of the tail only. Neither the RSS nor the SWS are visible on the UV photographs.

Technical data and quantities concerning the geometrical circumstances of the three red-light observations are summarized in Table 1, whereas reproductions of the corresponding plates are assembled in Fig. 1 so that the projection on the sky of the prolonged radius vector (the vector opposed with respect to the Comet-Sun one) is always pointing upward. The RSS is a prominent feature in these reproductions, whereas the SWS is hardly detectable, because of its faintness and of the greatly overexposed coma in which it is partly embedded. Image processing was necessary in order to emphasize this feature.

In the analysis of these features, we consider them as composed of dust. The spectral range of the observations is not sufficient, by itself, to assure this assumption, because some strong ion emissions can be detected also in red light: in Fig. 1 some rays probably due to the plasma are detectable, superimposed on the main dust tail. However, since the RSS does not appear in the UV plates, we should assume a periodical appearance of this

Table 1. Tautenburg red-light photographs of Comet Bennett 1970II. Technical data and geometrical quantities. Obs.: Serial number of the photographic plate. Date UT: May 1970 (mid-exposure). Exp.: Exposure time expressed in minutes. R.A., Decl.: Computed comet position. Δ, r: Earth-Comet and Sun-Comet distances. λ: Earth cometocentric latitude on the comet orbit plane. α: Phase angle. γ: Cometocentric angle between the Sun and the $-v$ directions

Obs.	Date UT	Exp.	R.A. (1950.0)	Decl. (1950.0)	Δ (AU)	r	λ	α	γ
3124	5.0663	35	$00^h51^m.26$	$+61°35'.2$	1.4614	1.1200	$+0°.1$	$43°.5$	$43°.9$
3125	7.0493	32	$01^h00^m.23$	$+62°19'.7$	1.5069	1.1527	$-1°.2$	$42°.0$	$41°.3$
3127	8.0490	45	$01^h04^m.68$	$+62°40'.5$	1.5296	1.1692	$-1°.8$	$43°.1$	$42°.8$

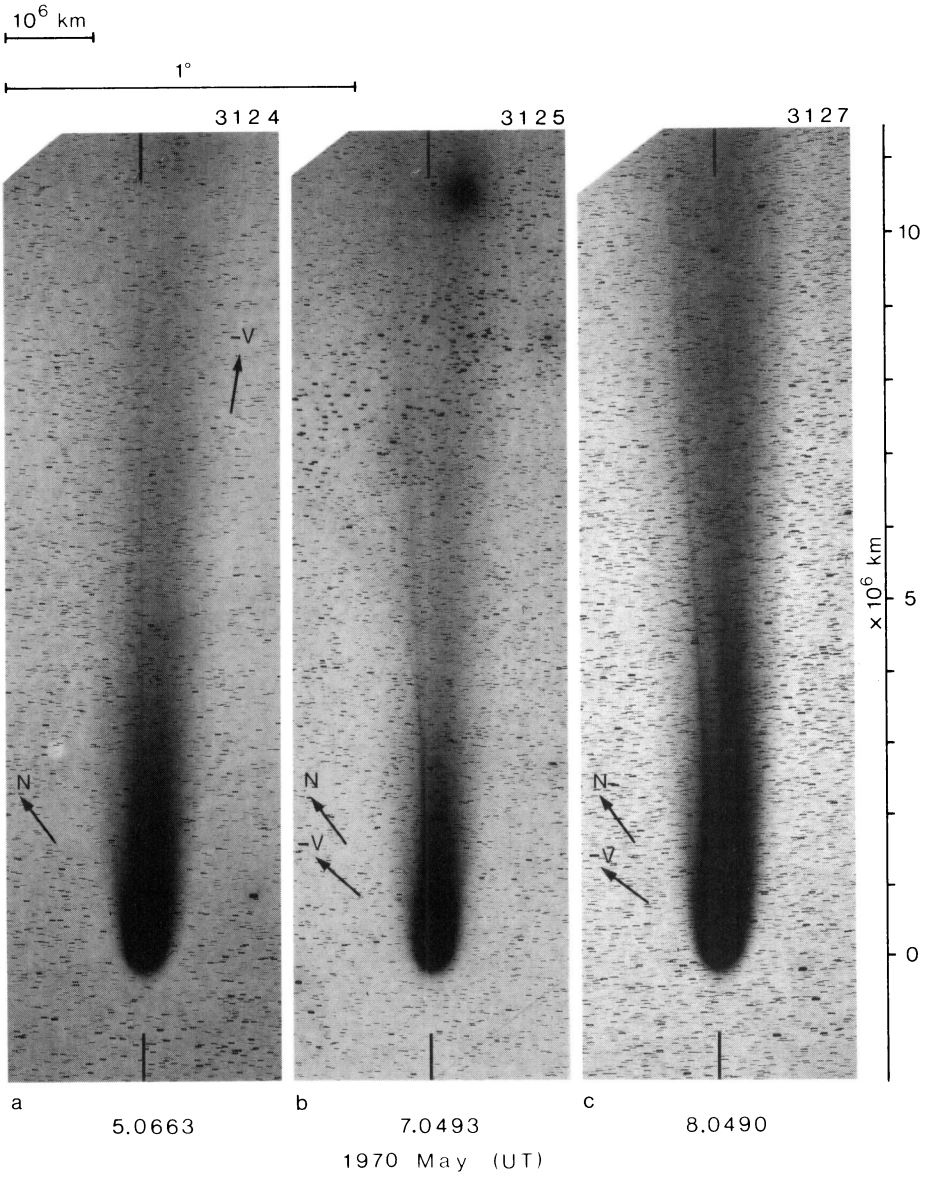

Fig. 1. Reproductions of the Karl Schwarzschild Observatory (Tautenburg) red-light plates of Comet Bennett 1970II (courtesy Prof. Richter). Each image is labeled with the original Tautenburg sequential number. Arrows N and $-V$ indicate the direction to the north through the nucleus and the direction of the projection on the sky of the comet negative velocity vector, respectively. Linear horizontal scale lies in the plane of the sky, whereas the vertical one represents the projection on the sky of a scale tilted to the line of sight as the observed RSS

hypothetical plasma feature during the red-light exposure and a disappearance during the UV ones. This seems to be quite improbable, on account of the very similar shape and position of the RSS during the three exposures, which allow us to consider it as the same structure observed at three different times. Moreover the formation of a plasma ray $\approx 10^7$ km long within a time interval of ≈ 1 h is inconsistent with the present knowledge about the formation, structure and kinematics of cometary Type I tails. The same arguments are even more plausible for the SWS, because a plasma structure of this kind was never detected.

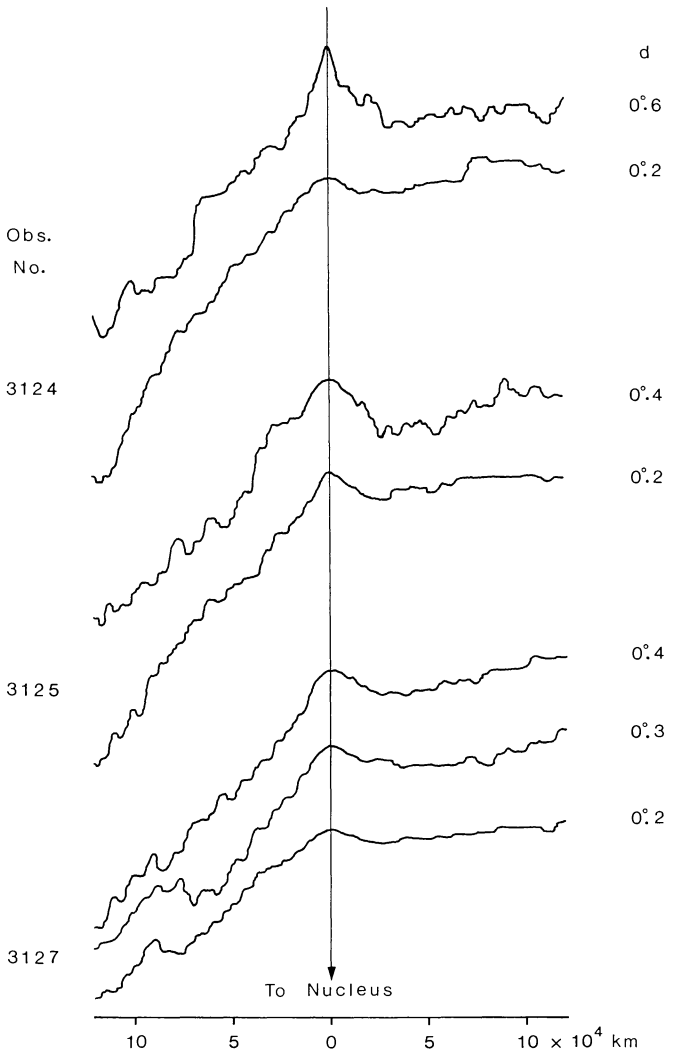

Fig. 2. Samples of the density profiles of the RSS. The angular distance from the nucleus of each scanning is denoted by *d*. Vertical line represents the axis of maximum density

2.2. *Geometrical circumstances*

The observing conditions of the tail are described by quantities λ, α, and γ in Table 1. The first represents the Earth cometocentric latitude, that is, the angle that the Comet-Earth vector makes with the plane of the comet orbit. It is positive when the Earth is in the comet north hemisphere. The other two quantities are the phase angle, and the angle in the comet orbit plane between the Sun-Comet radius vector and $-v$ (the negative velocity vector of the comet), respectively. All that these quantities say is:

(i) The Earth was extremely close to the plane of the comet orbit throughout the relevant time, hence the line of sight from the Earth to the comet was always nearly lying in the comet orbit plane. Under such projection conditions, any flat structure (thin layer of dust) confined to the plane of the comet orbit is expected to appear as a narrow and straight feature on the plane of the sky. The lower the cometocentric latitude of the Earth, the narrower and straighter (i.e. ray-shaped) the apparent structure. This is just the behaviour of the RSS in the photographs here collected (Fig. 1), if we observe them from right to left (i.e., with the time regressing and $\lambda \rightarrow 0$).

(ii) The Earth crossed the plane of the comet orbit shortly after observation 3124. According to Marsden's (1982) orbital elements, such an event occurred only 2.1 h later, on May 5.1548 UT. The passage of the Earth from one comet hemisphere to the other is expected to produce a rapid upsetting in perspective resulting in an apparent rotation of the tail about the comet head.

(iii) The Earth (or, more precisely, its projected position onto the comet orbit plane) was located very close to $-v$, but always in the sector defined by r and $-v$.

3. Reduction procedures

3.1. *The RSS feature*

In order to obtain precise position angles (PA's), we first tried measuring the position of the tail features directly on the plates (plan films), as for determining precise positions of minor planets and comets.

We soon realized however that such a method does not allow the precision required by our purposes, when applied to unsharp objects such as details in the comet tails. Thus, we analyzed the RSS by a microdensitometer in order to obtain sharp density profiles to be measured later for deriving the required PA's. The scanning was made in the direction perpendicular to the RSS, at different distances *d* from the nucleus. A sample of the obtained profiles is assembled in Fig. 2. They clearly show that, with the exception of the observation 3124, the density curves of the RSS are asymmetrical in shape, thus denoting that in observations 3125 and 3127 the axis of highest density was shifted toward the trailing (left in Figs. 1.3125 and 1.3127) boundary, that is the boundary facing the path of the orbit behind the nucleus. The measured and theoretical (following the model developed in Sect. 5) Position Angles (PA) of the RSS are shown in Table 2.

Table 2. Parameters of the RSS and SWS. Obs.: Serial number of the photographic plate. PA_{rss}: measured position angle of the RSS (error $\pm$ 0°.05). PA_{nl}: computed position angle of the Neck-Line. PA_{prv}: computed position angle of the prolonged radius vector. PA_{+v}: computed position angle of comet nucleus velocity vector. PA_{sws}: measured position angle of the SWS (error $\pm$ 0°.2). PA_{tss}: computed position angle of the SWS. *L*: measured projected length of the SWS (antitail)

Obs.	PA_{rss}	PA_{nl}	PA_{prv}	PA_{+v}	PA_{sws}	PA_{tss}	*L* (km)
3124	322°.96	322°.91	323°.02	133°.8	142°.8	142°.9	0.36 10^6
3125	325°.86	325°.90	323°.57	192°.2	145°.7	145°.6	0.35 10^6
3127	327°.26	327°.31	323°.82	196°.7	146°.7	146°.9	0.48 10^6

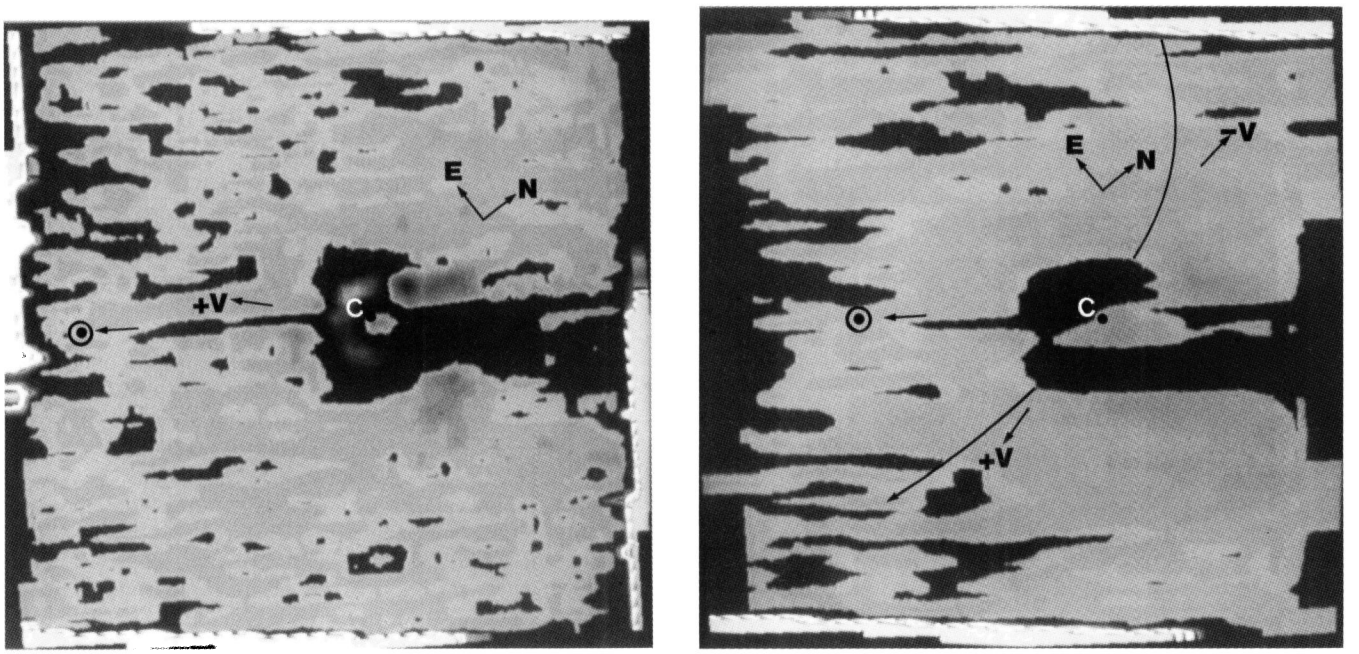

Fig. 3a and b. Difference of the intensity image and its median after directional filtering for observation 3124 (**a**) and 3127 (**b**). X-median filter size 21 pixels (**a**) and 61 pixels (**b**). Y-median filter size 11 pixels for both **a** and **b**. Arrows N, E, $+V$ and $\odot$ mark respectively the direction of the North and East starting from the nucleus, the projection on the sky of the comet positive velocity vector, and the Sun-comet radius vector. The curved line in **b** denotes the projection on the sky of the comet orbital path

3.2. The SWS feature

The procedure described above could not be applied to the SWS feature before enhancing it by means of image processing. The Tautenburg copies were digitized by means of a PDS 1010 A microdensitometer using a square aperture of $50\,\mu m \times 50\,\mu m$, a sampling step of $50\,\mu m$ both in the X and in Y directions, and a scanning format of 512×512 pixels centered approximatively on the comet nucleus. Since the noise is due mainly to the star trails, the signal to noise ratio resulted to be rather insensitive to the sampling procedure, whereas a too small sampling step would have greatly increased the computing difficulties of the numerical filtering needed to eliminate such noise.

The images, linearized into intensity by means of the calibration wedges available on the plates, were filtered by means of a symmetric median filter in order to estimate a pseudo-background. We subtracted to the intensity values of the original image those of the pseudo-background, thus obtaining difference images where the SWS was clearly visible but masked by the noise of the field star trails.

Since the SWS and the star trails happened to be nearly orthogonal, the difference images were used to define a directional filter specially made in order to enhance the antitail feature. This directional filter was implemented by means of a rotation, needed to align the SWS to the X axis, followed by a one-dimensional median filter of length matching the X-section width of the star trails applied to each row of the image, followed by another one-dimensional median filter of length matching the Y-section width of the star trails applied to each column of the image, and finally by the opposite rotation necessary to return to the original aspect of the images. The final images, on which the positional measurements were performed, are shown in Fig. 3 for observations 3124 and 3127.

The results of the measurements, concerning the parameter L (the projected maximum linear extension of the SWS detected on the images) and the measured and the theoretical Position Angles of the SWS following the model developed in Sect. 5, are summarized in Table 2.

4. Discussion of the results of data reduction

If we examine the photographs of Comet Arend-Roland 1957III (Sky and Telescope, 1957) taken between 1957 April 24 and 27 (the Earth crossed the comet orbital plane on 25.759 April 1957 UT), we can observe that the ray-shaped anti-tail shown by C/1957III has the same shape and time behaviour of the RSS of Comet C/1970II. These striking resemblances lead us to think that we might be in the presence of the same phenomenon, the different orientation of such features in the sky with respect to the Sun being a matter of different perspective only.

Most of the authors (e.g. Miller, 1957; Whipple, 1957) explained the sunward spike of Comet Arend-Roland as a thin layer of dust spread out in the plane of the comet orbit and viewed edgewise from the Earth. In order to account for such a sharp concentration of dust particles towards the plane, a special emission with very low ejection velocities from the inner coma occurring some time before the perihelion (Opik, 1958; Finson and Probstein, 1968b) was assumed. As to the greater sharpness and brightness of the trailing edge observed in the days before and after the Earth crossing, it was explained by Sekanina (1974) as caused by the tendency of the old synchrones to "pile-up" towards the earliest ejection times, with a consequent increase of density in coincidence with the trailing edge of the tail. This was then taken as the oldest synchrones, whose position denotes the onset time of appreciable dust production.

Kimura and Liu (1977) proposed an alternative interpretation, based on the Neck-Line Structures (NLS), which fitted closely the observations without introducing any special emission of dust particles with anomalous ejection velocities.

The NLS were found by Kimura and Liu (1977) in the development of their theoretical model of the dust tails of comets. In this model, each dust particle is taken as an infinitely small planetary body, whose orbital elements, and then its position in the space at any time, can be rigorously computed using keplerian orbit mechanics. Consequently, because of the keplerian motion of the individual particles, the initial spherical shells ejected from the nucleus (the Finson-Probstein model (1968a) of the inner coma is assumed) remain spherical for a while after emission, but soon they become ellipsoidal in shape, by collapsing onto the orbital plane of the parent comet at the second node of the particles orbits, that is, at the point π away in true anomaly from the point of ejection (the first node). At the second node, the original spherical shells will be completely flattened on the plane of the comet orbit. The resulting flat structure of particles of different sizes and different emission times, that cross the comet orbital plane (each in its second node) at a given instant of time is called the Neck-Line Structure (NLS) for this instant.

The geometrical conditions under which a NLS can be observed in a well developed tail are essentially two:

(i) The comet must have passed its perihelion.

(ii) The Earth must be close to the plane of the comet orbit.

The first condition is imposed by the spatial location of the second node of the particle orbits. As to the second one, the resulting edgewise (or near edgewise) perspective allows a better visibility of the NLS, which should appear as a bright and narrow ray surrounded by a fainter, more or less wide envelope representing the edgewise projection on the sky of the three-dimensional part of the tail, that is, of the collapsing ellipsoids composed by dust ejected with continuity by the comet nucleus. Both the above conditions are satisfied in the observations of Comet Arend-Roland, as well as in the observations of Comet Bennett here collected.

Both the interpretations of Sekanina (1974) and Kimura and Liu (1977) account for the Comet Bennett RSS observations. However the Kimura and Liu model avoids unrealistic hypotheses on the dust ejection velocities. Moreover the interpretation of the SWS of the same comet will support strongly the Kimura and Liu model with respect to that of Sekanina.

The SWS of Comet Bennett 1970II seems to be a structure intrinsically different from the antitails observed in other comets. See for example the compilation by Sekanina (1976), including eight comets, and the comets Bradfield 1975XI (Sekanina and Pansecchi, 1977), Cernis-Petrauskas 1980k (Everhart, 1980) and Austin 1984i (Emerson, 1984). In all these cases the perspective was the only cause of the phenomenon since the particles of those perspective antitails were located outside the path of the comet orbit. On the contrary, in the case of Comet Bennett 1970II there are observational evidences that the particles of the antitail were located inside the path of the comet orbit ahead of the nucleus with respect to the Sun:

(i) The SWS was located in the sector defined by the Sun-Comet radius vector and the comet velocity vector $+v$ along the sunward prolongation of the RSS, and therefore it does not satisfy the criterion by Sekanina (1976) which must be verified in the case of the appearance of a perspective antitail.

(ii) The drawing of the orbital path of the comet nucleus shows that in all the three observations the SWS was located effectively inside the orbit of the comet (see the evident example in Fig. 3b).

This allows us to exclude the SWS be a perspective dust formation and to consider such structure as a real antitail in the Bredikhin sense (Jaegermann, 1903).

Several hypotheses can be considered in order to account for this feature, but most of them result quite impracticable. We neglect possible electromagnetic effects that might arise from the interaction of charged dust with the solar wind, which are inadequate to justify the length and the orientation of the SWS. Also the hypothesis of the dragging out of dust by the expanding gas should be rejected, because too high velocities should be needed in order to account for the SWS length, which would turn out incompatible with the high collimation of the spike.

Let us consider the Sekanina model of the RSS: the only way of obtaining the SWS within this hypothesis is to assume an ejection of very large grains (which do not suffer the radiation pressure) with high velocity in the comet orbital plane (in order to account for the length of the SWS) and with a much lower velocity out of the comet orbital plane (in order to account for the high collimation of the SWS and of the RSS). This could be only caused by the presence on the comet nucleus (characterized by a spin axis perpendicular to its orbital plane) of an unique small source of dust located in the equatorial plane. This model of the comet nucleus seems to be quite artificial, and it is not supported by any direct observation.

Instead, it will be shown in the next section that the NLS model account for both the RSS and the SWS. The length of the SWS will allow us to compute the ejection velocity of the largest dust grains.

5. The Neck Line Structures

We are interested in the time when the dust ellipsoids, after having collapsed, are completely flattened onto the plane of the comet orbit at a point π away in true anomaly from the ejection point. It is possible to reconstruct the shape of the resulting flat ellipses by considering only the motion of the particles ejected from the nucleus along the orbital plane of the comet coincident with the orbital plane of the particles. This allows us to reduce the equations of motion of the dust grains in terms of only three geometrical orbital parameters, namely (1) the eccentricity e_d, (2) the perihelion distance q_d, and (3) the perihelion orientation θ_d with respect to that of the comet orbit. Therefore the dust grain orbit will be, in polar coordinates (r, v):

$$r = q_d(1 + e_d)/[1 + e_d \cos(v - \theta_d)]. \quad (1)$$

We consider the motion of a dust grain as a function of four variables, three of which are independent, namely (1) the radial ejection velocity v_e of the dust grain related to the comet nucleus, (2) the angle φ_e between the direction of the ejection and the subsolar point (this angle is measured in the plane of the comet orbit; it is zero in coincidence with the subsolar point, and corotates with the anomaly of the comet nucleus), (3) the time interval $\tau = t_c - t_e$ between the dust ejection time t_e and the observation time t_c, and (4) the effective gravity force parameter $\mu = 1 - F_{rad}/F_{grav}$ acting on the dust grain (F_{rad} is the solar radiation force and F_{grav} is the solar gravity force). Finally, let us denote the eccentricity and the perihelion distance of the comet orbit respectively by e_c and q_c.

Following Finson and Probstein (1968a), let be M, N the rectangular coordinates in the plane of the sky, with the origin in the comet nucleus, where M is the prolonged Sun-Comet radius

vector. The coordinates M, N of a dust grain at the time t_c can be expressed as follows:

$$\begin{aligned} &M = M(v_e, \varphi_e, \tau, \mu; t_c), \\ &N = N(v_e, \varphi_e, \tau, \mu; t_c), \\ &f(v_e, \varphi_e, \tau, \mu) = 0, \end{aligned} \tag{2}$$

where the third equation is a constraint imposed so that the system (2) corresponds to a NLS. The tie consists in the fact that the anomaly of every particle placed in a point given by (2) has to be $v_e + \pi$, where v_e is the anomaly of the dust grain at the ejection time t_e. This requires an equation for v_e that can be expressed as a function of τ. The tie equation is:

$$\begin{aligned} &t(v_e + \pi - \theta_d, e_d, q_d, \mu) - t(v_e - \theta_d, e_d, q_d, \mu) \\ &\quad + t(v_e, e_c, q_c, 1) - t(v_c, e_c, q_c, 1) = 0, \end{aligned} \tag{3}$$

where v_c is the comet nucleus true anomaly at the time t_c and t is the time function:

$e < 1$

$$\begin{aligned} \psi(v, e) &= \sqrt{[(1-e)/(1+e)]}\, \tan(v/2) \\ t(v, e, q, \mu) &= 2(\mu G \mathcal{M})^{-1/2}\, [q/(1-e)]^{3/2} \\ &\quad \cdot \{\tan^{-1} \psi(v, e) - e\, \psi(v, e)/[1 + \psi^2(v, e)]\} \\ t(v, 1, q, \mu) &= [2/(\mu G \mathcal{M})]^{1/2}\, q^{3/2}\, [\tan(v/2) + \tan^3(v/2)/3] \end{aligned} \tag{4}$$

$e > 1$

$$\begin{aligned} \psi(v, e) &= \sqrt{[(e-1)/(e+1)]}\, \tan(v/2) \\ t(v, e, q, \mu) &= 2(\mu G \mathcal{M})^{-1/2}\, [q/(e-1)]^{3/2} \\ &\quad \cdot \{\ln\{[1 - \psi(v, e)]/[1 + \psi(v, e)]\} \\ &\quad + e\, \psi(v, e)/[1 - \psi^2(v, e)]\} \end{aligned}$$

where $\mathcal{M}$ is the Sun mass and G is the gravitational constant.

We have to solve the Eq. (3) for v_e by iterations. The dust grain orbital parameters are functions of the variables $v_e, \varphi_e, \tau, \mu$ and so of v_e too:

$$\left.\begin{aligned} &e_d(v_e, \varphi_e, \tau, \mu) \\ &= \sqrt{\{1 + [a(v_e, \varphi_e, \tau, \mu) - 2/r_e(\tau)]\, b(v_e, \varphi_e, \tau, \mu)\}} \\ &q_d(v_e, \varphi_e, \tau, \mu) \\ &= b(v_e, \varphi_e, \tau, \mu)/[1 + e_d(v_e, \varphi_e, \tau, \mu)] \\ &\theta_d(v_e, \varphi_e, \tau, \mu) \\ &= v_e - \sin^{-1} \frac{q_d(v_e, \varphi_e, \tau, \mu)\, [1 + e_d(v_e, \varphi_e, \tau, \mu)]\, w_x(v_e, \varphi_e, \tau)}{r_e(\tau)\, e_d(v_e, \varphi_e, \tau, \mu)\, w_y(v_e, \varphi_e, \tau)} \\ &\theta_d(v_e, \varphi_e, \tau, \mu) \\ &= v_e - \cos^{-1} \frac{q_d(v_e, \varphi_e, \tau, \mu)\, [1 + e_d(v_e, \varphi_e, \tau, \mu)] - r_e(\tau)}{r_e(\tau)\, e_d(v_e, \varphi_e, \tau, \mu)}, \end{aligned}\right\} \tag{5}$$

where we have used the auxiliary parameters

$$\left.\begin{aligned} &r_e(\tau) = q_c(1 + e_c)/[1 + e_c \cos v_e(\tau)] \\ &w_x(v_e, \varphi_e, \tau) = \sqrt{\{G\mathcal{M}/q_c(1+e_c)\}}\; e_c \sin v_e(\tau) - v_e \cos \varphi_e \\ &w_y(v_e, \varphi_e, \tau) = \sqrt{\{G\mathcal{M}/q_c(1+e_c)\}}\, [1 + e_c \cos v_e(\tau)] - v_e \sin \varphi_e \\ &a(v_e, \varphi_e, \tau, \mu) = [w_x^2(v_e, \varphi_e, \tau) + w_y^2(v_e, \varphi_e, \tau)]/\mu G \mathcal{M} \\ &b(v_e, \varphi_e, \tau, \mu) = r_e^2(\tau)\, w_y^2(v_e, \varphi_e, \tau)/\mu G \mathcal{M}. \end{aligned}\right\} \tag{6}$$

By solving Eq. (3) we impose the constraint $f(v_e, \varphi_e, \tau, \mu) = 0$ and thus the value of τ is determined by the value of $v_e = \boldsymbol{v}_e$ that satisfies Eq. (3), as follows:

$$\tau = t(\boldsymbol{v}_e + \pi - \theta_d, e_d, q_d, \mu) - t(\boldsymbol{v}_e - \theta_d, e_d, q_d, \mu) \tag{7}$$

Substituting in (1) the $\boldsymbol{v}_e$ value, we obtain the NLS point in the orbit plane (r, v) reached by the dust grain after the time τ. Since in our case the NLS extension is negligible with respect to the Earth-Comet distance, we can project this point on the sky plane by means of a rotation matrix in order to obtain the coordinates (2). By varying the values of the variables v_e, φ_e and μ, the Eq. (3) is satisfied by different values of v_e. In this way we obtain the dependence of the coordinates (M, N) upon the fourth variable τ.

It is useful to consider the families of curves that can be obtained from system (2) when we fix two of the three independent variables. The diagram in Fig. 4, which refers to observation 3127, is intended to illustrate these curves as they appear in the comet orbit plane.

When we fix the μ and v_e parameters, we introduce the isotachy locus, which will be characterized by dust grains ejected from the inner coma with the same velocity v_e and by true anomalies different among them, but all equal to the starting one of the specific grain plus π. The isotachies represent the contour lines of the ellipsoidal dust shells collapsed onto the comet orbit plane. In the limit case of $v_e = 0$, and with the parameter μ free, we obtain the locus of the centers of the isotachies, that is the Neck-Line introduced by Kimura and Liu (1977).

When we fix the μ and τ parameters, we introduce the isochrona locus (not to be confused with the Bredikhin synchrones). Here the isochrones are nothing but the nodal lines of the particle orbits. All the particles along a given isochrone have been ejected from the inner coma at the same time $t_c - \tau$ and therefore have the same true anomaly equal to the starting one (v_e) plus π, whenever is the value of μ.

If we consider the projection of these loci in the sky plane, it is possible to obtain analytical expressions which introduce negligible errors with respect to the rigorous numerical ones. The M axis (the prolonged radius vector projected on the sky plane) is the origin of the polar angle $\Omega = \Omega(\varphi_e)$, which is a function of φ_e that we can compute by solving the Eq. (3) for $v_e = \text{const}$ and $0 < \varphi_e < 2\pi$. The analytical expressions of the loci considered are:

Neck-Line:

$$\begin{aligned} M(\mu) &= (1 - \mu)\, s \cos(\Omega_\tau + \Omega_\mu) \\ N(\mu) &= (1 - \mu)\, s \sin(\Omega_\tau + \Omega_\mu), \end{aligned}$$

Isochrone:

$$N(\tau) = c(\tau - \tau_0),$$

Isotachy:

$$\begin{aligned} M(\varphi_e; v_e, \mu) &= F(\varphi_e)\, v_e \cos \Omega(\varphi_e) + (1 - \mu)\, s \cos(\Omega_\tau + \Omega_\mu) \\ N(\varphi_e; v_e, \mu) &= F(\varphi_e)\, v_e \sin \Omega(\varphi_e) + (1 - \mu)\, s \sin(\Omega_\tau + \Omega_\mu) \\ F(\varphi_e) &= \{[a \cos(\Omega(\varphi_e) - \Omega_\tau)]^2 \\ &\quad + [b \sin(\Omega(\varphi_e) - \Omega_\tau)]^2\}^{-1/2}, \end{aligned}$$

(8)

where the introduced parameters (shown and defined in Table 3 for the observations considered here) can be obtained by solving Eq. (3) iteratively. Equations (8) can be used to build up the NLS for any observation time. The NLS will become to be the envelope of all the isotachies (for any μ-value) characterized by suitable v_e-values, which will be functions of μ.

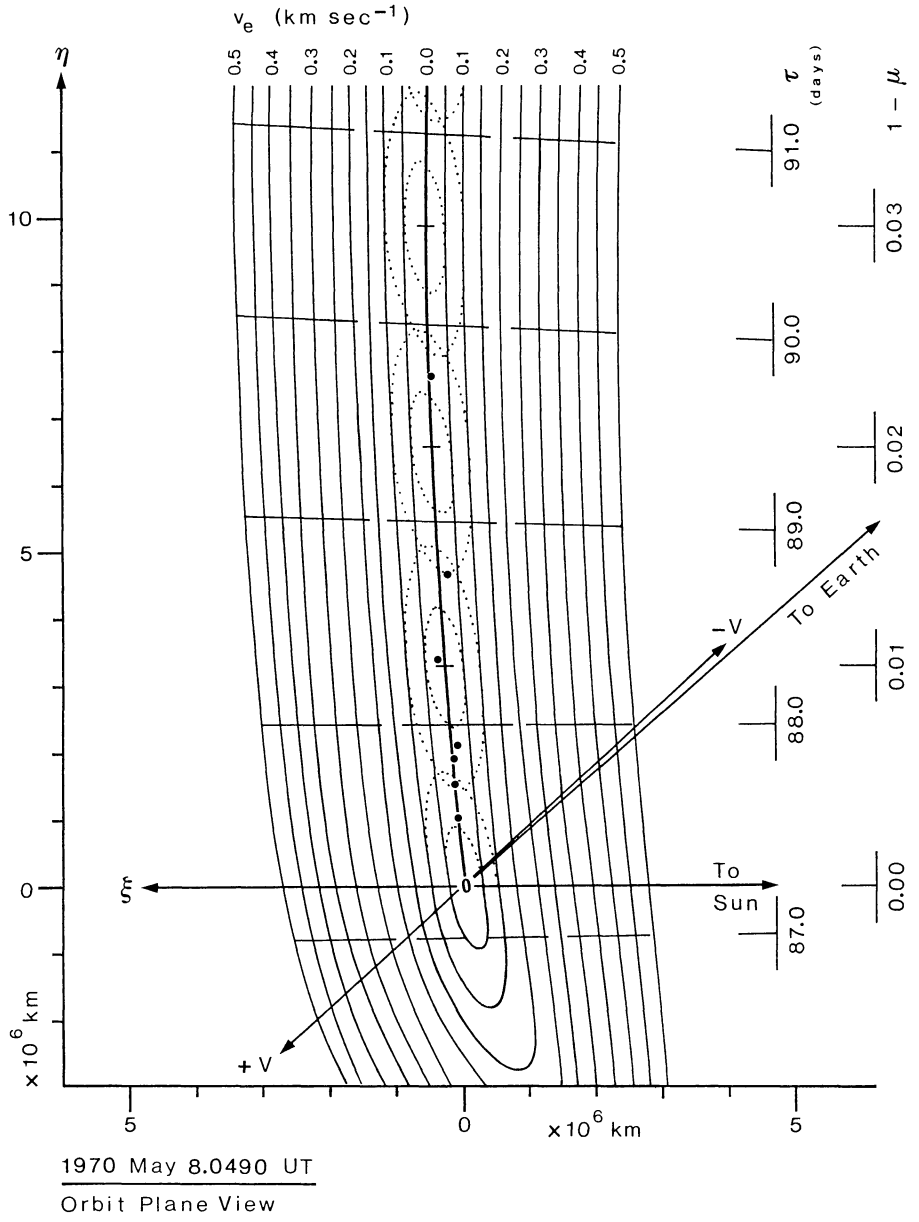

Fig. 4. Orbit plane view of the isochrones (dashed lines) and the isotachies (dotted lines) for observation 3127. Arrows $+V$ and $-V$ denote the positive and negative velocity vectors of the comet nucleus (indicated with an unfilled dot). The thin solid lines are the envelopes of the isotachies (dotted ellipses), i.e. hypothetical NLS's for μ-independent v_e values. The heavy solid line connecting the centers of the isotachies is the Neck-Line introduced firstly by Kimura and Liu (1977). The solid dots along such a line represent the projected relevant points measured by means of the microdensitometer along the axis of highest density of the RSS. Note that $v_e \geqq 0.03\,\mathrm{km\,s^{-1}}$ is required in order to obtain the observed length L of the SWS (Table 2). See text for the definition of the other symbols

Table 3. Parameters of the loci of the NLS. Obs.: Serial number of the photographic plate. a: inverse of the isotachy major semiaxis. b: inverse of the isotachy minor semiaxis. c: length parameter of the isochrones. s: length parameter of the Neck-Line. τ_0: isochrone passing through the comet nucleus. Ω_τ: polar angle of the isotachy major axis with origin along M axis. $\Omega_\tau + \Omega_\mu$: polar angle of the Neck-Line with origin along M axis

Obs.	$a\,(\mathrm{s^{-1}})$	$b\,(\mathrm{s^{-1}})$	$c\,(\mathrm{cm\,s^{-1}})$	$s\,(\mathrm{cm})$	τ_0 (days)	Ω_τ	Ω_μ
3124	$6.165\ 10^{-8}$	$2.5\ 10^{-5}$	$0.045\ 10^{5}$	$2.403\ 10^{13}$	86.5920	−0°.09	−0°.02
3125	$6.017\ 10^{-8}$	$5.9\ 10^{-6}$	$1.130\ 10^{5}$	$2.537\ 10^{13}$	86.9866	+2°.01	+0°.32
3127	$5.945\ 10^{-8}$	$4.3\ 10^{-6}$	$1.790\ 10^{5}$	$2.605\ 10^{13}$	87.2478	+3°.04	+0°.45

6. Application of the model

In Sect. 3.1, we measured the position angle of the axis of highest density of the RSS. In the NLS hypothesis, it should coincide with the axis of the isotachies, that is the Neck-Line. Therefore we have to compare PA_{rss} with PA_{nl}, obtained by adding to the PA_{prv} value (the position angle of the M axis) the angle $\Omega_\tau + \Omega_\mu$ in Table 3, obtained from expression (8). The results are shown in Table 2, in good agreement with the observations.

Having some concern, however, that such a close fit might be only determined by the strong foreshortening effect, we projected the measured relevant points of the RSS onto the comet orbit plane (Bernasconi and Bernasconi, 1966) in order to compare their position with respect to the Neck-Line also in such a plane. We consider only observation 3127, utilizing the diagram in Fig. 4. It shows clearly that the projected relevant points (solid dots) are very close to the Neck-Line also in the comet orbit plane.

The dust ellipsoids composed by the largest dust grains, on which the radiation pressure force has negligible effects, after having collapsed on the comet orbital plane, will form a flat ellipse approximately centered on the comet nucleus. Therefore half of this ellipse will be placed in the inner part of the comet orbit, thus resulting in a real antitail. Moreover it will appear as a sunward spike seen edgewise when the Earth will be placed in the comet orbit plane.

The theoretical Position Angles PA_{tss} of the SWS, obtained by adding the quantities $\Omega_\tau + \pi$ (see Table 3) to the quantities PA_{prv}, are shown in Table 2. We find a good agreement between these theoretical values and the quantities PA_{sws} determined from the observations (Sect. 3.2).

The dust ejection velocity from the inner coma has to satisfy the observed length of the SWS. In fact the sunward extension in the comet orbit plane of the NLS is given by the size of the isotachies, which is ruled by the v_e variable. We follow the Probstein's results (1969) about the μ-dependence of v_e, which can be summarized, following Finson and Probstein (1968b) and Kimura and Liu (1977), as follows, where the parameter k can be considered $0.0 < k < 0.5$:

$$v_e = v_0 (1-\mu)^k . \tag{9}$$

The link between the SWS length L and v_e must satisfy:

$$F(1-\mu) = L + (1-\mu)\, s - (1-\mu)^k\, v_0/a = 0 . \tag{10}$$

From the derivative of F we deduce that F has a minimum for

$$1-\mu = (v_0\, k/a\, s)^{1/(1-k)} \tag{11}$$

thus allowing us to search the solution of (10) for the value $1-\mu$ given by (11). Since the variation of the geometrical parameters used in (10) for the three observations available is very low, we can consider them as constants. The result of the computations is shown in Fig. 5 for different values of L. Taking a Sun-Comet distance of about 1 AU, as in our case, the previous determinations of v_0 and k yield values of $v_0 = 0.5\ \mathrm{km\,s^{-1}}$ (Finson and Probstein, 1968b) or $v_0 = 0.6\ \mathrm{km\,s^{-1}}$ (Sekanina and Miller, 1973), and $k = 0.2 \div 0.5$. If we put these values in Fig. 5, we obtain a length L of the SWS very close to that really observed (see Table 2).

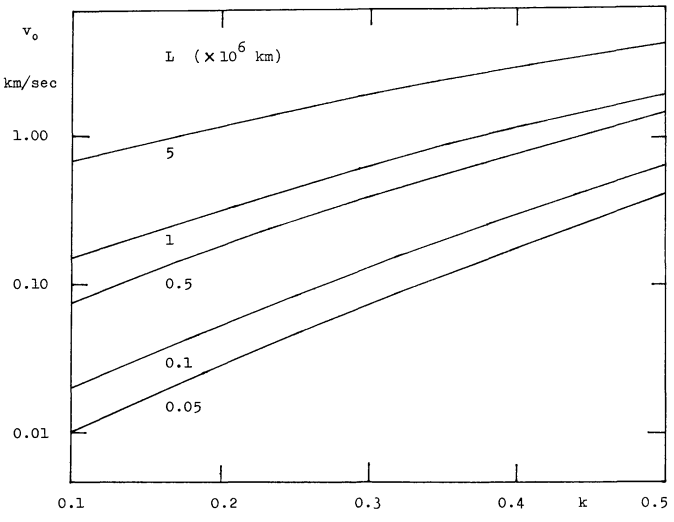

Fig. 5. Theoretical solutions for different values of the length L of the real dust antitail measured in 10^6 km unit

7. Conclusions

The rigorous treatment of the motion of the dust grains composing the Type II tail of comets allowed Kimura and Liu (1977) to obtain the theoretical formulation of the Neck-Line Structures. However, a decisive proof about their effective existence was never reached. These structures can be detected only under perspective conditions so severe that no discriminating criterion with respect to the usual model of the meteoric swarm was obtained up to now.

In this paper, the detection of two anomalous structures in the tail of Comet Bennett 1970II is reported. The only plausible explanation of their composition is dust, so providing an opportunity to apply a new complete formulation of the NLS model. The observed position of the ray-shaped structures fits closely the position computed by the model. However, this close fitting is not sufficient, by itself, to exclude the Sekanina's interpretation of the ray-shaped structures of comet dust tails.

The observation of the sunward spike offers the discriminating criterion between the two models. The NLS model explains both the anomalous features of the dust tail of Comet Bennett without introducing unrealistic hypotheses on the dust ejection velocity and the nucleus topography, which are necessary when we follow the Sekanina model.

Having shown, by means of pure astrometric methods, that the most suitable model for the anomalous structures of the dust tail of Comet Bennett is the NL is important, because the photometric analysis of the same features will allow to apply the quantitative treatment of the NLS and to obtain new results on the dust physics of Comet Bennett (Fulle and Sedmak, 1986).

However, some informations about the dust composing the NLS can be deduced from the results obtained in this paper. From the length of the RSS visible on the plates ($\approx 11\ 10^6$ km), it follows that the dust grains have a $1-\mu$ value between $0 < 1-\mu < 0.04$ (parameter s in Table 3) and were emitted from the inner coma between 3 and 10 Feb 1970 (parameters τ_0 and c in Table 3). The same conclusions about the sizes and ejection times of the RSS dust would equally result from the Sekanina model (meteoric swarm). The only difference between the two interpretations is the following: the Sekanina model implies that the RSS dust is the oldest dust ejected from the comet nucleus at about zero velocity, whereas the NLS model implies that dust older than the RSS one was ejected before 3 Feb, and with non-zero velocity with respect to the comet nucleus.

With regard to the dust production rate from the comet nucleus required to obtain the observed RSS and SWS, a dust emission limited between the isochrona values covered by the NLS would be sufficient. However, this artificial hypothesis can be avoided. We can consider a continuous and uniform dust production for a time interval much longer than the one covered by the NLS. In this case, the dust ellipsoids flattened onto the NLS will be surrounded by the collapsing ellipsoids, that is, by a dust halo, effectively observed in the collected photographs.

Acknowledgements. We wish to dedicate the present paper to the memory of Prof. Dr. Nikolaus Benjamin Richter (died on 1980 November 26), who supplied us with fine duplicates of the original plates taken at the Karl Schwarzschild Observatory, Tautenburg. Further, we are indebted to: A. Bernasconi, who discussed with the first author about some geometrical aspect of the problem; E. Colombini (Osservatorio San Vittore, Bologna), who helped us in the astrometric reduction of the plates; and M. Scardia (Osservatorio Astronomico di Brera, Milano-Merate), who assisted us in the use of the microdensitometer to obtain the density profiles. The photographic material was digitized on the PDS 1010A microdensitometer at Trieste Astronomical Observatory. The image processing was made on the Astronet Trieste VAX/750 system using also UK Starlink software. P. Santin of Trieste Astronomical Observatory is the author of the magnetic tape software and standard file software used in this work. L. Lampi and M. Quartana of Trieste Astronomical Observatory helped us in producing the photographs shown in this paper. We thank the unknown referee for having pointed out unclear physical discussions in the early version.

References

Bernasconi, G., Bernasconi, A.: 1966, *Mem. Soc. Astron. Ital.* **37**, 647
Emerson, G.: 1984, *Sky Tel.* **68**, 482
Everhart, E.: 1980, *Sky Tel.* **60**, 474
Finson, M.L., Probstein, R.F.: 1968a, *Astrophys. J.* **154**, 327
Finson, M.L., Probstein, R.F.: 1968b, *Astrophys. J.* **154**, 353
Fulle, M., Sedmak, G.: 1986, *Astron. Astrophys.* (submitted)
Högner, W., Richter, N.: 1980, *Isophotometric Atlas of Comets*, Part II, Springer, Berlin, Heidelberg, New York
Jaegermann, R.: 1903, Prof. Dr. Th. Bredikhin's Mechanische Untersuchungen über Cometenform, St. Petersburg
Kimura, H., Liu, C.-P.: 1977, *Chin. Astron.* **1**, 235
Marsden, B.G.: 1982, *Catalogue of Cometary Orbits*, 4th edition, Central Bureau for Astronomical Telegrams, Cambridge, Mass.
Miller, F.D.: 1957, *Sky Tel.* **16**, 365
Miller, F.D., Blanco, V.M., Gomez, A.: 1971, *Publ. Astron. Soc. Pacific* **83**, 216
Opik, E.J.: 1958, *Irish A.J.* **5**, 37
Probstein, R.F.: 1969, in *Problems of Hydrodynamics and Continuum Mechanics*, ed. M.A. Lavrent'ev, Philadelphia, p. 568
Sekanina, Z.: 1974, *Sky Tel.* **47**, 374
Sekanina, Z.: 1976, in *The Study of Comets*, eds. B. Donn et al., NASA SP-393, p. 893
Sekanina, Z., Miller, F.D.: 1973, *Science* **179**, 565
Sekanina, Z., Pansecchi, L.: 1977, *Astrophys. Letters* **18**, 61
Sky and Telescope (1957) **16**, 412
Whipple, F.L.: 1957, *Sky Tel.* **16**, 426